Undersea & Hyperbaric Medicine, Vol. 20, No. 3, 1993

Relationship between venous bubbles and hemodynamic responses after decompression in pigs

A. VIK, B. M. JENSSEN, O. EFTEDAL, and A.-O. BRUBAKK

Section for Extreme Work Environment, Sintef Unimed, 7034 Trondheim, and Department of Biomedical Engineering, University of Trondheim, Medical University Center, 7005 Trondheim, Norway

Vik A, Jenssen BM, Eftedal O, Brubakk AO. Relationship between venous bubbles and hemodynamic responses after decompression in pigs. Undersea & Hyperbaric Med 1993; 20(3):233–248.—We present a new pig model for studying relationships between venous gas bubbles and physiologic effects during and after decompression. Sixteen pigs were anesthetized to allow spontaneous breathing. Eight of them underwent a 30-min exposure to 5 bar (500 kPa) followed by a rapid decompression to 1 bar (2 bar/min); the remaining eight served as controls. The pigs were monitored for intravascular bubbles using a transesophageal echocardiographic transducer, and bubble count in the two-dimensional ultrasound image of the pulmonary artery was used as a measure of the number of venous gas bubbles. Effects on physiologic variables of the pulmonary and the systemic circulations were either measured or estimated. We detected venous bubbles in all pigs after decompression, but the inter-individual variation was large. The time course of changes in the mean pulmonary artery pressure, in the pulmonary vascular resistance, in the arterial oxygen tension, and in the pulmonary shunt fraction followed the time course of the bubble count. In contrast, such a relationship to the number of venous gas bubbles was not found for the immediate increase in mean arterial pressure and for the changes in the other variables of the systemic circulation. We conclude that the number of venous gas bubbles, as evaluated by the bubble count in the ultrasound image of the pulmonary artery, is clearly related to changes in the variables of the pulmonary circulation in this pig model.

swine, decompression sickness, air embolism, pulmonary circulation, echocardiography

Venous gas bubbles are known to be formed in divers during or after many decompressions (1–3). Such bubbles may be "silent" and induce no acute symptoms (3), or they may induce symptoms of DCS. However, it is also possible that silent bubbles can induce minor damage in tissues and result in long-term effects in divers (4). Regarding DCS, the precise cause of the disease is unknown, but it is clear that the pathogenesis proceeds via the formation of an endogenous gas phase. Thus, to elucidate the importance of venous gas bubbles in the pathogenesis of DCS as well as in the development of any long-term effects in divers, the relationship between the amount of gas that appears as bubbles in the venous circulation and physiologic responses is an important issue.

Many decompression experiments using different animal models have been performed during the last century, but monitoring of the hemodynamic effects in larger-sized animals has only been done in a limited number of studies (1, 5–11). Symptoms of DCS such as paresis, "chokes," or death have been used as an endpoint, and usually the amount of venous gas emboli in the pulmonary circulation has been unknown.

To study the relationship between intravascular gas bubbles formed during decompression and their physiologic responses, reliable systems for determining the presence and quantities of intravascular gas bubbles are required. Doppler instruments are by far the most common application of ultrasound for bubble detection (1, 12). However, it has been argued that ultrasound imaging may have several advantages in the detection (1) and possibly in the quantification of intravascular gas bubbles (12, 13).

In this study, we present a pig model for investigating the occurrence of venous gas bubbles and the physiologic responses of decompression stress. This species was chosen because certain cardiopulmonary similarities between the pig and the human have been pointed out (14, 15). The young pig (>2 mo.) has a lung circulation morphologically similar to that of adult humans (16), and the pig seems to respond to exercise in the same way that humans do with regard to oxygen consumption and cardiac output (17, 18). We have developed a method for estimating relative quantities of gas bubbles in the venous circulation of the pig by counting bubbles in the ultrasound image of the pulmonary artery (19). These bubble counts were related to changes in physiologic variables, something that has not been reported previously.

MATERIALS AND METHODS

Surgical procedure

Sixteen domestic farm swine (2–3 mo. old, body weight 19.5–29 kg) were used as experimental animals. The pigs were fasted for 16 h with free access to water. Fifteen to twenty minutes before induction of anesthesia, the pigs received premedication; 7–9 mg/kg azaperonum (Stresnils, Janssen) were injected intramuscularly. Atropinsulfat (1 mg, Atropin, Hydro Pharma) was thereafter given intravenously via an ear vein, and anesthesia was induced by thiopental sodium (5 mg/kg, Thiopenton Natrium, Nycomed Pharma) and ketamine (20 mg/kg, Ketalar, Parke Davis) maintained by a continuous i.v. infusion of ketamine in 0.9% NaCl (30 $mg \cdot kg^{-1} \cdot h^{-1}$). A tracheotomy was performed, whereafter the pigs were in the supine position, breathing spontaneously through an endotracheal tube. Body temperature was monitored by a rectal probe and maintained at 37.5°–38.5°C using a heating pad during surgery. During the dive the temperature inside the chamber was regulated (29.5°–30.5°C). Since a superficial, irregular respiratory pattern was observed approximately 30 min after anesthesia was induced, a bolus dose of α-chloralose in 0.9% NaCl (10–15 mg/kg, 0.25% solution, Sigma, St. Louis, MO) was injected intravenously. One or two supplemental doses were usually injected during the following 30 min to achieve a more regular respiratory rate. It was necessary, however, to restrict the dose to avoid CO_2 tensions above 6 kPa in the arterial blood (20). During the rest of the experimental period, no supplemental doses of α-chloralose were

injected because the anesthetic is known to have a longlasting effect (21). After the injection of the α-chloralose solution, the ketamine infusion provided the pigs with i.v. fluid at a rate of approximately 3–4 ml · kg^{-1} · h^{-1}.

Two polyethylene catheters (0.76 mm i.d.) were introduced into the left jugular vein and moved into the pulmonary artery to measure pulmonary arterial pressure and to obtain mixed venous blood for gas analysis. A third catheter was positioned in the right atrium via the right jugular vein for measurement of central venous pressure. Two polyethylene catheters (1.14 and 0.76 mm i.d.) were inserted into the right femoral artery and advanced into the abdominal aorta for continuous monitoring of arterial pressure and to obtain samples for analysis of blood gas composition.

Measurements and calculations

All intravascular pressures were recorded on a Grass polygraph (model 7D, Grass Instrument Co, Quincy, MA) using transducers (Sorensen Transpac II, Abbott Laboratories), which were calibrated against a mercury manometer, with zero pressure referred to the left ventricular mid-level. Calculations of mean pulmonary arterial pressure (PAP), mean arterial pressure (MAP), and mean central venous pressure (CVP) in millimeters of mercury, and calculation of heart rate (HR, beats/min) were made after the experiments.

Arterial and mixed venous blood were analyzed for P_{O_2} and P_{CO_2} using an IL 1306 pH/blood gas analyzer (Instrumentation Laboratories), and the blood gases were corrected for changes in rectal temperature using standard methods. Further, hemoglobin (Hb, g/100 ml), $\%O_2Hb$ (% of oxyhemoglobin), and %COHb (% of carboxyhemoglobin, *see Eq.6*) for calculating content of oxygen were measured using an IL 482 CO-Oxymeter (Instrumentation Laboratories). Oxygen content in arterial (Ca_{O_2}, ml/100 ml) and mixed venous (Cv_{O_2}) blood was calculated according to the equation:

$$Ca_{O_2} \text{ (or } Cv_{O_2}) = (1.53 \cdot Hb \cdot \frac{\%O_2Hb}{100}) + (P_{O_2} \cdot 0.003) \quad (1)$$

where 1.53 (ml/g) is the oxygen transport capacity of 1 g of pig hemoglobin [calculated from data given by Hannon et al. (22)]; and (P_{O_2} · 0.003) is the amount of oxygen (ml/100 ml) physically dissolved in the plasma.

Estimates of pulmonary blood flow ($\dot{Q}$, ml · kg^{-1} · min^{-1}) were made using the direct Fick method:

$$\dot{Q} = \frac{\dot{V}_{O_2}}{Ca_{O_2} - Cv_{O_2}} \quad (2)$$

where $\dot{V}_{O_2}$ is the oxygen consumption (ml · kg^{-1} · min^{-1}) calculated according to the equation (23):

$$\dot{V}_{O_2} = \dot{V}_E \cdot \frac{FI_{O_2} - FE_{O_2}}{[(1 - FI_{O_2}) + RQ \cdot (FI_{O_2} - FE_{O_2})] \cdot BW} \quad (3)$$

$\dot{V}_E$ (ml · min^{-1}, converted to standard conditions after the experiment, STPD) is the expiratory flow; FI_{O_2} and FE_{O_2} are the O_2 fractions of the inspiratory and expiratory air, respectively; RQ is the respiratory quotient, assumed to be 0.90; and BW is the body weight of the pig. The $\dot{V}_E$ was measured by a flow transducer head (Fleisch

no. 2) connected to a two-way valve located at the proximal end of the endotracheal tube. By means of thin-gauge polyethylene tubing, the alternating differential pressure was fed to a pneumotachograph (Gould Godart), and $\dot{V}E$ was recorded continuously on the Grass polygraph (except during the chamber dive). The pigs breathed room air during the experiment, and the FI_{O_2} was analyzed before the experiment by sampling a fraction of room air, drying it using Silica gel, removing CO_2 by the use of a CO_2 absorbent (Ascarite), and passing it into an oxygen analyzer (S3A, Applied Electrochemistry). FE_{O_2} was measured continuously during the experiment (except during the chamber dive) by sampling a fraction of the respiratory gas from the expiratory tubing. The values were recorded on a chart writer (Watanabe Servocorder, SR 6310).

The total pulmonary shunt fraction was calculated using the equation:

$$\dot{Q}_s/\dot{Q}_t = \frac{Cc_{O_2} - Ca_{O_2}}{Cc_{O_2} - Cv_{O_2}} \quad (4)$$

where $\dot{Q}_s$ = shunt flow and $\dot{Q}_t$ = flow through the pulmonary system. Cc_{O_2} (end-capillary oxygen content, ml/100 ml) was calculated according to the equation:

$$Cc_{O_2} = (1.53 \cdot Hb \cdot K) + (0.0031 \cdot PA_{O_2}) \quad (5)$$

where

$$K = (1 - \frac{\%COHb}{100}) - 0.02 \quad (6)$$

for $PA_{O_2} < 125$ mmHg. PA_{O_2} (alveolar tension of O_2, mmHg) was estimated as:

$$PA_{O_2} = [FI_{O_2} \cdot BP] - [Pa_{CO_2} \cdot (FI_{O_2} + \frac{1 - FI_{O_2}}{RQ})] \quad (7)$$

where BP is the barometric dry pressure.

In estimating pulmonary vascular resistance (PVR, mmHg · ml^{-1} · kg · min), left atrial pressure was assumed to be zero.

$$PVR = PAP/\dot{Q} \quad (8)$$

Systemic vascular resistance (SVR, mmHg · ml^{-1} · kg · min) was estimated as:

$$SVR = (MAP - CVP)/\dot{Q} \quad (9)$$

Bubble detection

A transesophageal echocardiographic (TEE) probe (6.5 MHz) interfaced with a CFM 750 color flow scanner (Vingmed, Horten, Norway) was inserted and positioned to obtain a simultaneous two-dimensional view of the pulmonary artery and the aorta (24). The ultrasound images were stored on videotape during the compression and decompression periods, as well as during the following 90 min. Digitized images were transmitted at regular intervals from the CFM scanner to a Macintosh II computer. These images were subsequently processed using a software program for

automatic quantification of the number of gas bubbles (19) (Fig. 1). Thus, a relative estimate of the amount of venous gas bubbles in the pulmonary artery was obtained.

The minimum size of a bubble that could be automatically detected and counted was not limited by the software program, but by the ultrasound equipment, because no information was lost in the process of digitizing and transferring the images to the computer. Small-sized gas bubbles ($\leq$50 μm) have been injected into a hydromechanical simulator of the cardiovascular system and detected and counted after transmission of digitized images (19). We do not know exactly the detection threshold of the TEE probe used in this study, but most likely it detects gas bubbles far below 50 μm (24, 25). We had technical problems with the penetrator in the chamber in one of the first experiments in this study, allowing no accurate counting of the bubbles in the ultrasound image. However, the TEE probe has provided a high-quality image of the pulmonary artery in >97% of our subsequent pig experiments.

Experimental procedure

After surgery, the pigs were placed inside a chamber (300 liter) specially constructed to fit pigs of this size. At least 30 min were needed for stabilization, and predive data were collected at 20 min and at 3–5 min before compression started.

Eight pigs [decompression group, BW 22.8 kg (SD 2.0)] underwent a 30-min exposure to 5 bar (500 kPa) (compression rate 2 bar/min), followed by a rapid decompression to 1 bar (2 bar/min). Bottom time was calculated from the beginning of compression to the beginning of decompression. The pigs were breathing chamber air during the experimental dive, and soda lime was placed inside the chamber to prevent an increase of CO_2 in the chamber atmosphere. Continuous monitoring of gas bubbles in the pulmonary artery and of intravascular pressures was carried out during the dive, using special chamber connectors. Data were collected immediately after surfacing, and then every 5th min during the initial 30 min after decompression. Thereafter measurements were made at 15-min intervals, with the final measurement made after 90 min. The first values for $\dot{Q}_s/\dot{Q}_t$, $\dot{Q}$, PVR, and SVR were calculated 5 min after surfacing. After the experiments, the hearts of all the pigs were investigated at autopsy; none of the animals had a patent foramen ovale.

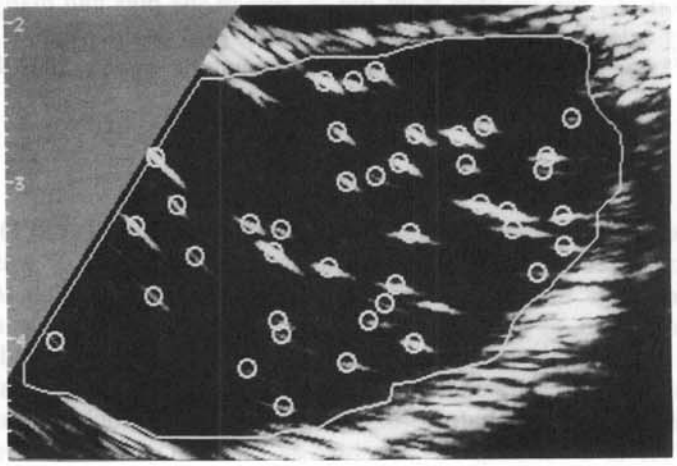

FIG. 1—Ultrasound image of the pulmonary artery in one pig after decompression. Gas bubbles have been detected (*circles*) and counted automatically after transmission to a Macintosh II computer.

Eight additional pigs served as controls [control group, BW 23.6 kg (SD 2.9)]. They were subjected to a procedure identical to that of the decompression group, except that they underwent no compression. Data measurements were obtained at the same intervals as those for the pigs exposed to pressure. The observation period was 110 min, which corresponds to the period from −50 to 60 min postdecompression for the decompression group.

Statistics

Data were analyzed on a Macintosh computer (Stat Works version 1.2, Cricket Software Inc., Philadelphia, PA). Maximum and minimum values of each variable were compared with the base-line values for any significant effects, using paired Student's t test. Furthermore, the times taken to reach maximum change from base line were calculated (26). In the control group, base-line values were compared with the corresponding values at the end of the observation period using paired Student's t test. Spearman's rank correlation was used for analysis of correlation. Because many variables were tested, $P < 0.01$ was defined as the level of significance; $0.01 < P < 0.05$ indicated a tendency, although no significant effect could be shown. Values are presented as means (95% confidence interval, CI) in the text, in the tables, and in figure 4.

RESULTS

Formation of gas bubbles

Gas bubbles appeared in the pulmonary artery in all pigs. We usually detected the first bubbles during the last 10–15 s of the decompression (at approximately 1.5 bar) or immediately after "surface" was reached. The relative bubble count increased rapidly during the ensuing period, to reach a maximum at 21 min (95% CI 13 to 29) (Fig. 2). Thereafter the bubbles decreased in number, but it was still possible to observe venous gas bubbles 90 min after decompression in all pigs. The time to reach maximum value of the bubble count was chosen so that no increase >10% occurred during the following period. As can be seen from Fig. 2, five of the pigs had many bubbles in the pulmonary artery, whereas the two remaining pigs (no. 29 and 31) generated considerably fewer bubbles (range of maximum bubble count: 58–338 bubbles $\cdot s^{-1} \cdot cm^{-2}$).

Hemodynamic responses

Pulmonary arterial pressure increased rapidly after decompression (Table 1). Ninety minutes after decompression, PAP had returned to predive values or was lower than predive values. The time course of the PAP changes was related to changes in relative bubble counts, as demonstrated in Fig. 2. A correlation between time to reach maximum PAP and time to reach maximum bubbles was observed, although it was not significant ($r_s = 0.80$, $P = 0.033$, $n = 7$). However, in most pigs, the highest PAP values appeared before the highest number of bubbles was counted. An increase in PAP of ≤1 mmHg was accepted as a normal variation when

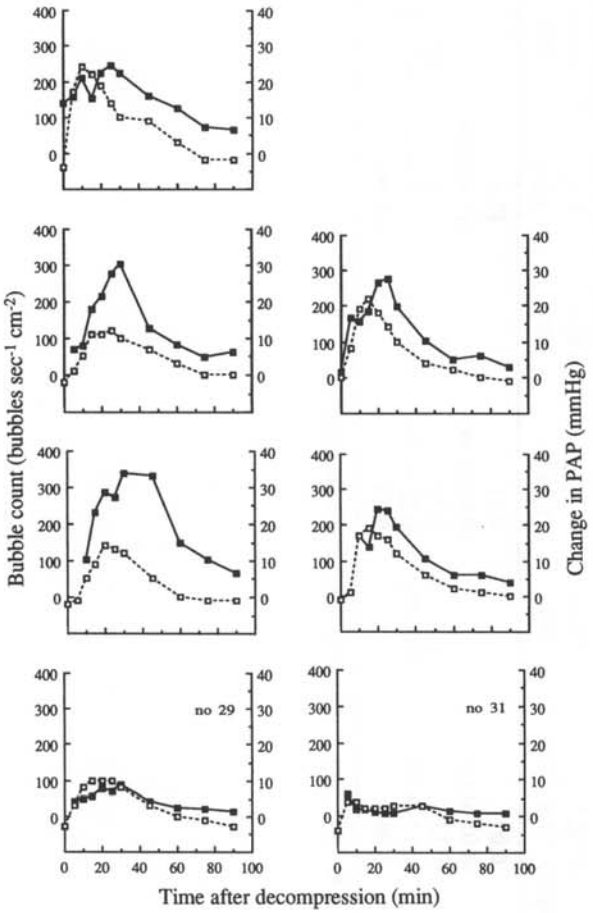

FIG. 2—Bubble formation after decompression as evaluated by bubble counts in a two-dimensional image of the pulmonary artery in seven pigs. Time course of bubble count (*solid squares*) is plotted together with the corresponding changes in the PAP (*open squares*) in each pig, i.e., changes from the predive values.

choosing the maximum value of PAP. Although there seemed to be a relationship between the maximum bubble count and the corresponding change in PAP, as demonstrated in Fig. 2, no significant correlation was observed ($r = 0.43$, $P = 0.34$, $n = 7$), which could be due partly to small sample size.

The other variables of the pulmonary circulation, $\dot{Q}_s/\dot{Q}_t$ and Pa_{O_2} (Fig. 3) and PVR, also showed a time-dependent response similar to that observed for the bubble count. It should be noted that the Pa_{O_2} values were very high and showed wide variations immediately after the chamber dive (13.9–23.6 kPa) due to the high P_{O_2} tension in the chamber and probably to differences in the ventilatory pattern during the last period of the hyperbaric exposure.

Central venous pressure increased rapidly to reach peak values (Table 2), followed by a decrease below predive values. Similarly, MAP increased in all pigs to reach maximum values (Fig. 4). A decrease below predive values was thereafter observed. In contrast, $\dot{Q}$ values tended to be reduced compared to the predive values when MAP reached its maximum. SVR was therefore significantly higher than it was before the dive. SVR thereafter decreased and stabilized at a level between the peak and the predive values, whereas $\dot{Q}$ remained low throughout the experiment. No changes in HR could be detected.

Table 1: Hemodynamic variables of the pulmonary circulation in eight pigs before and after decompression[a]

Point of Time	PAP, mmHg	Time, min	PVR,[b] $mmHg \cdot ml^{-1} \cdot kg^{-1} \cdot min^{-1}$	Time, min	$\dot{Q}s/\dot{Q}t$[c]	Time, min	Pa_{O_2}, kPa	Time, min
Baseline	15.5		0.07		0.11		12.6	
(95% CI)	(12.4–18.6)		(0.05–0.09)		(0.08–0.14)		(11.6–13.6)	
Max. response	32.0	14	0.18	16	0.39	18	7.9	20
(95% CI)	(25.3–38.7)	(10–18)	(0.14–0.22)	(10–22)	(0.22–0.56)	(15–21)	(5.9–9.9)	(17–23)
P	0.001		0.003		0.006		<0.001	

[a]Values are means and 95% confidence interval. [b]$n = 6$. Time, time in minutes to reach maximum response; [c]$n = 7$.

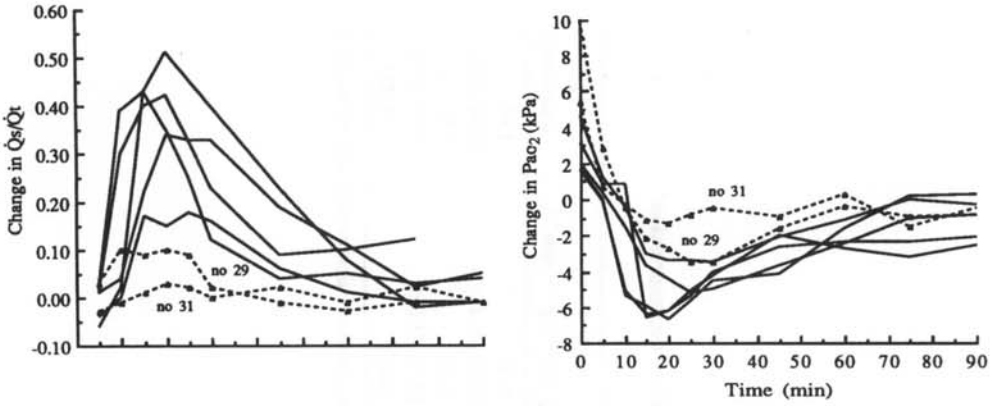

FIG. 3—Change in shunt fraction ($\dot{Q}_s/\dot{Q}_t$) and in arterial O_2 tension (Pa_{O_2}) (i.e., from predive values) after decompression in seven pigs in which bubbles were counted. Few bubbles were counted in pigs 29 and 31.

Control group

The measured and calculated physiologic variables in the control group remained stable throughout the 110-min observation period (Table 3). However, the $\dot{Q}_s/\dot{Q}_t$ demonstrated a tendency to decrease, and the SVR tended to increase slowly.

DISCUSSION

We have presented a pig model that allowed us to do a relative estimation of the number of gas bubbles that entered the pulmonary circulation after decompression. Furthermore, this estimate of venous gas bubbles could be related to physiologic effects. If we assume there is a relationship between the occurrence of DCS and the total gas loading in the body, and possibly the amount of gas that enters the pulmonary artery as gas bubbles (27), this model can be of great value in further research on decompression-related problems.

Responses to gas bubbles in the pulmonary circulation

We expected the pigs to generate venous gas bubbles because a severe decompression profile had been chosen in this experiment. However, in two of the pigs, very few bubbles were detected. Thus, the great variation in the degree of bubble formation observed in our eight pigs accords with the individual variability in endogenous gas generation found in humans (3).

The results clearly demonstrated relationships between the time course of the bubble count and the time course of the changes in PAP. During air infusion, a relationship has been shown to exist between the infusion rate and the rate of increase in PAP (24, 28). Furthermore, maximum PAP values have been shown to be dose-related up to a threshold above which PAP does not increase any further (29, 30). Since the number of gas bubbles that enters the pulmonary circulation after decompression is time-dependent, it is difficult to extrapolate the results from studies on continuous air infusion to explain effects caused by decompression. It is likely,

Table 2: Hemodynamic variables of the systemic circulation in eight pigs before and after decompression[a]

Point of Time	CVP, mmHg	Time, min	MAP, mmHg	Time, min	$\dot{Q}$,[b] ml·kg^{-1}·min^{-1}	SVR,[b] mmHg·ml^{-1}·kg^{-1}·min^{-1}	HR, beats/min
Baseline	1.8		85		204	0.37	130
(95% CI)	(0.9–2.7)		(75–95)		(166–242)	(0.27–0.47)	(104–156)
Max. response	2.9	9	101	11	177	0.53	131
(95% CI)	(0.9–4.9)	(7–11)	(88–114)	(8–14)	(141–213)	(0.41–0.65)	(107–155)
P	0.058		0.011		0.033	0.009	0.911

[a]Values are means and 95% CI. Time, time to reach maximum response. Values for $\dot{Q}$, SVR, and HR are those measured or calculated at time of maximal MAP response. [b]$n = 6$.

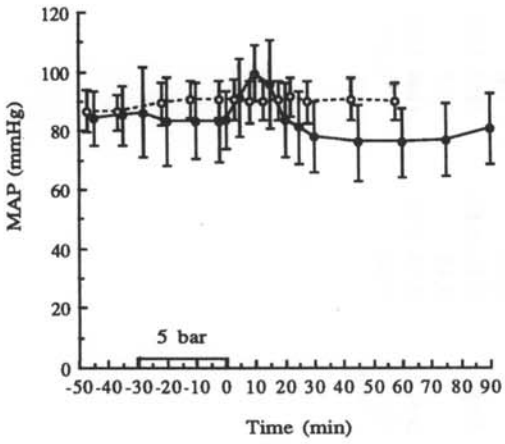

Fig. 4—Effects of rapid decompression on MAP for the eight pigs in the decompression group (*solid circles*). Control group underwent no compression (*open circles*, $n = 8$). For clarity, the values presented in the figures for the control group are 2 min later than those actually recorded at the times shown. *Error bars* = 95% CI.

however, that a relationship exists between the number of venous gas emboli and PAP changes after decompression. The rate of increase in PAP, the maximum PAP value, and the rate of decrease in PAP are therefore probably related to the amount of gas that appears as bubbles in the pulmonary circulation.

In the two pigs in which few bubbles were detected, we observed a small increase in PAP, whereas a larger increase in PAP was observed in the pigs that had many bubbles in the pulmonary artery. These findings suggest that the bubble count in the ultrasound image can be used as an indication of the amount of gas that appears as venous bubbles in different individuals. One should note, however, that a considerable range of individual PAP changes occur during continuous air infusion, in spite of using the same infusion rate (24, 30). The correlation between the dose of venous gas bubbles and PAP changes in a single individual is therefore not sufficiently close to allow accurate prediction, even when the amount of gas that enters the pulmonary circulation as bubbles is known. In addition to low sample size, this latter fact could explain why we did not find a significant correlation between maximum bubble count and the corresponding PAP changes.

Interestingly, maximum values of PAP were reached before maximum bubble count in most of the pigs. In several pigs, the PAP had started to decrease when the number of gas bubbles seemed to be at its highest. We suggest that vasoconstriction in the pulmonary vasculature contributed to the rapid increase in PAP during the initial 20 min after decompression. In most of the pigs, a small decrease in all three intravascular pressures was observed during compression. A high Pa_{O_2} during compression may induce a relative vasodilation in the pulmonary vasculature and thereby reduce the PAP (31). Vasoconstriction in the pulmonary circulation after decompression could be secondary to this "hyperoxic vasodilation." However, the relationship between bubble count and PAP changes (Fig. 2), as well as the correlation between time to reach maximum bubble count and time to reach maximum PAP, suggests that gas bubbles in the pulmonary circulation contributed to the major increase in the PAP.

It is well documented that gas emboli, in addition to obstructing the pulmonary vasculature mechanically, induce vasoconstriction either by the release of mediators or by activating reflex mechanisms (32). Small-sized bubbles (<170 μm) are more likely to induce vasoconstriction than larger-sized bubbles (33). In dogs, it was found

Table 3: Hemodynamic variables of eight control pigs at base line and at the end of the observation period (110 min)[a]

Point of Time	PAP, mmHg	PVR,[b] mmHg·ml^{-1}·kg^{-1}·min^{-1}	$\dot{Q}s/\dot{Q}t$[b]	Pa_{O_2}, kPA	CVP, mmHg	MAP, mmHg	$\dot{Q}$,[b] ml·kg^{-1}·min^{-1}	SVR,[b] mmHg·ml^{-1}·kg^{-1}·min^{-1}	HR, beats/min
Baseline	16.0	0.07	0.20	12.0	1.6	87	233	0.37	126
(95% CI)	(15.0–17.0)	(0.06–0.08)	(0.12–0.28)	(10.2–13.8)	(0.5–2.7)	(80–94)	(180–286)	(0.30–0.44)	(102–150)
110 min	15.5	0.08	0.16	12.3	1.7	90	215	0.44	117
(95% CI)	(13.1–17.9)	(0.06–0.10)	(0.08–0.24)	(10.8–13.8)	(0.8–2.6)	(83–97)	(142–288)	(0.34–0.54)	(104–130)
P	0.598	0.220	0.021	0.431	0.785	0.288	0.079	0.026	0.316

[a]Values are means and 95% CI. [b]$n = 7$.

that the inert gas bubbles increased in size during the initial 25-min period after decompression (34). We suggest that the rapid increase in PAP in our pigs, that occurred immediately after surfacing, was caused by small-sized bubbles that induced vasoconstriction. During the following period, larger-sized bubbles probably induced less vasoconstriction, and the PAP could actually decrease despite an increasing number of bubbles.

Changes in the other three variables of the pulmonary vasculature, PVR, Pa_{O_2}, and $\dot{Q}_s/\dot{Q}_t$, were also related to bubble count. The $\dot{Q}_s/\dot{Q}_t$ ratio, or shunt fraction, describes the fraction of blood that is passing through unventilated areas from the right to the left of the heart, and the $\dot{Q}_s/\dot{Q}_t$ and Pa_{O_2} values are usually related (31). During pulmonary microembolization, collapsed lung units probably induce an increase in $\dot{Q}_s/\dot{Q}_t$ (32). Inasmuch as none of the pigs had a patent foramen ovale, this can be excluded as a factor contributing to the increase in $\dot{Q}_s/\dot{Q}_t$ (32). The course of these three variables supports the finding of a relationship between the number of gas bubbles after decompression, as evaluated by bubble count in the ultrasound image, and effects on the pulmonary circulation.

Responses in the systemic circulation

Central venous pressure and MAP values increased after decompression and returned to base line when the bubble count reached maximum. SVR and $\dot{Q}$ did not show the same relationship to the bubble count as the four variables of the pulmonary circulation did. An activation of the sympathetic nervous system or a release of vasoactive substances could explain the sudden increases in MAP and SVR values and the decrease in $\dot{Q}$ values. Bove et al. (6) speculated that the rise in systemic resistance observed in their dogs could be due to obstruction of peripheral vascular beds by local bubble formation or bubble emboli. We know that only two of our pigs had arterial gas bubbles that had escaped pulmonary filtration (35), but the increases in MAP and SVR were observed in all eight pigs. A rapid increase in plasma catecholamines has been observed after decompression in dogs (8), and no increase in MAP was reported, but data were not presented for the period when MAP and SVR peaked in the present study. Since the changes in MAP, SVR, and $\dot{Q}$ observed in our study are compatible with the effects of norepinephrine on the systemic circulation (36), we could speculate that a release of catecholamine may contribute to the effects we report.

During air infusion in mechanically ventilated pigs, we demonstrated a decrease in MAP, and a small decrease was observed in the present pigs after the MAP had reached peak values and returned to base-line values (Fig. 4). The secondary decrease in MAP was therefore most likely an effect of venous gas emboli, whereas the immediate increase could be an effect of both the decompression and the gas bubbles.

In the control pigs we observed that both the measured and the calculated values of most monitored variables remained very stable throughout the 110-min observation. When anesthetized, spontaneously breathing animals are used in experimental studies, atelectasis of the lungs and thereby reduced alveolar ventilation and increased $\dot{Q}_s/\dot{Q}_t$ ratio may be a complication (31). The opposite situation was observed in our pigs, namely a tendency for the $\dot{Q}_s/\dot{Q}_t$ to decrease, which indicates a satisfactory ventilation in the pig model. Although there was a tendency for SVR to increase

slowly in the control pigs, this cannot explain the rapid change in SVR in the decompression group, where the SVR curves peaked 5–15 min after decompression.

It has often been argued that use of the direct Fick method for measuring $\dot{Q}$ requires the existence of stable conditions during the last 3 min before sampling (31). However, if an oxygen analyzer is used to measure oxygen consumption continuously, 30–45 s may be sufficient for stabilization after circulatory and respiratory changes (37). The main source of error during an unsteady state is changes in pulmonary ventilation (37). Unpublished data show a small increase in ventilation during the initial 15 min after decompression in our pigs, which may have resulted in an overestimation of $\dot{V}O_2$ and $\dot{Q}$. Thus, both the decrease in $\dot{Q}$ and the increase in SVR calculated at maximum MAP may have been underestimated.

Studies on sheep (1, 5, 11), dogs (6–9), and goats (10) have also been performed to elucidate physiologic effects after rapid decompressions. In these studies, different animal models and different dive profiles were used, so it is difficult to directly compare the observed effects. The study by Bove et al. (6) on anesthetized, spontaneously breathing dogs exposed to 8 bar (40–60 min) followed by rapid decompression seemed to demonstrate qualitatively the same hemodynamic effects as observed in our pigs. Right ventricular pressure, PVR, CVP, MAP, and SVR all increased, whereas $\dot{Q}$ and Pa_{O_2} decreased. An exception was the HR, which increased in their dogs but not in our pigs.

Method of detection and quantification of gas bubbles

In most of the above-mentioned studies in other animal species (1, 5, 6, 10, 11), ultrasound Doppler was used to detect bubbles. Powell et al. (1) tried to estimate the amount of gas that appeared as bubbles after decompression by comparing the increase in right ventricular systolic pressure (RVSP) with the increase in RVSP observed during venous air infusion at different rates. From this comparison they suggested the dose of gas after decompression at which the different Doppler grades occurred (Spencer's 0–4 scale). Atkins et al. (5) also presented Doppler results, using Spencer's code and mean effects of the physiologic variables, whereas D'Aoust et al. (10) indicated a relationship between the increase in bubble count as measured by Doppler and the decrease in mixed venous N_2 content.

The use of two-dimensional imaging and a software program for automatic counting of bubbles in the pulmonary artery introduces new possibilities for quantification of the venous bubbles arising during and after decompression (19). One major advantage over Doppler grading methods is that the two-dimensional imaging requires little previous training, whereas training is required for the use of Doppler grade analysis (38). Better spatial resolution suggests that the scanning method is more sensitive than the Doppler method (Fig. 1). Finally, the ultrasound imaging method gives an objective, continuous, and linear scale of the number of intravascular gas bubbles detected. The Doppler gradings are somewhat subjective, and the relationship between the grades and the number of gas bubbles is non-linear. Furthermore, the grading scale is not continuous. Using two-dimensional imaging, the occurrence of arterial gas bubbles can also be monitored simultaneously (1, 24, 35)

The disadvantage of the two-dimensional imaging system is that the equipment is more expensive and complicated and less portable than the Doppler system. It should be noted that two-dimensional imaging only permits approximate quantification of

the amount of gas that enters the pulmonary vasculature as gas bubbles, because the images do not cover the whole pulmonary artery and no attempts have been made to estimate the size of the detected bubbles. Despite these limitations, a TEE transducer is a valuable tool for detection and semiquantification of gas bubbles when anesthetized animals are used in decompression-related research.

We thank A. Sira for development of chamber instrumentation and H. Kvithyll and I. Hansen at the Animal Laboratory of the Trondheim Regional and the University Hospital for their help.

This study has been supported financially by Statoil and Phillips Petroleum, Norway. Some of these results were presented at the XVIIth Annual Meeting of EUBS on Diving and Hyperbaric Medicine, Crete, Greece, 29 September to 3 October 1991, and published in the proceedings.—*Manuscript received September 1992; accepted March 1993.*

REFERENCES

1. Powell MR, Spencer MP, von Ramm O. Ultrasonic surveillance of decompression. In: Bennett PB, Elliott DH, eds. The physiology and medicine of diving, 3d ed. San Piedro, CA: Best Publishing, 1982:404–434.
2. Eckenhoff RG, Parker JW. Latency in onset of decompression sickness on direct ascent from air saturation. J Appl Physiol 1984; 56:1070–1075.
3. Eckenhoff RG, Olstad CS, Carrod G. Human dose-response relationship for decompression and endogenous bubble formation. J Appl Physiol 1990; 69:914–918.
4. Elliott DH. Long-term sequelae of diving. J R Soc Med 1989; 82:79–80.
5. Atkins CE, Lehner CE, Beck KA, Dubielzig RR, Nordheim EV, Lanphier EH. Experimental respiratory decompression sickness in sheep. J Appl Physiol 1988; 65:1163–1171.
6. Bove AA, Hallenbeck JM, Elliott DH. Circulatory responses to venous air embolism and decompression sickness in dogs. Undersea Biomed Res 1974; 1:207–220.
7. Catron PW, Flynn ET, Yaffe L, et al. Morphological and physiological responses of the lungs of dogs to acute decompression. J Appl Physiol 1984; 57:467–474.
8. Catron PW, Thomas LB, McDermott JJ, et al. Hormonal changes during decompression sickness. Undersea Biomed Res 1987; 14:331–341.
9. Catron PW, Thomas LB, Flynn ET, McDermott JJ, Holt MA. Effects of He–O_2 breathing during experimental decompression sickness following air dives. Undersea Biomed Res 1987; 14:101–111.
10. D'Aoust BG, Swanson HT, White R, Dunford R, Mahoney J. Central venous bubbles and mixed venous nitrogen in goats following decompression. J Appl Physiol 1981; 51:1238–1244.
11. Neuman TS, Spragg RG, Wagner PD, Moser KM. Cardiopulmonary consequences of decompression stress. Respir Physiol 1980; 41:143–153.
12. Brubakk AO. Ultrasonic methods for detection of gas bubbles. In: Brubakk AO, Hemmingsen BB, Sundnes G, eds. Supersaturation and bubble formation in fluids and organisms. Trondheim, Norway: Tapir Publishing, 1989:353–385.
13. Ikeda T, Suzuki S, Shimizu K, Okamoto Y, Llewellyn ME. M-mode ultrasonic detection of microbubbles following saturation diving: a case report and proposal for a new grading system. Aviat Space Environ Med 1989; 60:166–169.
14. Dodds WJ. The pig model for biomedical research. Fed Proc 1982; 41:247–256.
15. Douglas WR. Of pigs and men and research: a review of applications and analogies of the pig, *Sus scroa*, in human medical research. Space Life Sci 1972; 3:226–234.
16. Rendas A, Branthwaite M, Reid L. Growth of pulmonary circulation in normal pig: structural analysis and cardiopulmonary function. J Appl Physiol 1978; 45:806–817.
17. Sanders M, White F, Bloor C. Cardiovascular responses of dogs and pigs exposed to similar physiological stress. Comp Biochem Physiol A Comp Physiol 1977; 58:365–370.
18. Hastings AB, White FC, Sanders TM, Bloor CM. Comparative physiological responses to exercise stress. J Appl Physiol 1982; 52:1077–1083.
19. Eftedal O, Brubakk AO. Detecting intravascular gas bubbles in ultrasonic images. Med & Biol Eng & Comput 1993; in press.
20. Svendsen P, Ainsworth M, Carter A. Acid-base status and cardiovascular function in pigs anaesthetized with α-chloralose. Scand J Lab Anim Sci 1990; 17:89–95.

21. Green CJ. Animal anaesthesia. London: Laboratory Animal Ltd, 1982:81.
22. Hannon JP, Bossone CA, Wade CE. Normal physiological values for conscious pigs used in biomedical research. Lab Anim Sci 1990; 40:293–298.
23. Withers PC. Measurement of $\dot{V}O_2$, $\dot{V}CO_2$ and evaporative water loss with a flow-through mask. J Appl Physiol 1977; 42:120–123.
24. Vik A, Brubakk AO, Hennessy TR, Jenssen BM, Ekker M, Sløndahl SA. Venous air embolism in swine: transport of gas bubbles through the pulmonary circulation. J Appl Physiol 1990; 69:237–244.
25. Vik A, Jenssen BM, Brubakk AO. Effect of aminophylline on transpulmonary passage of venous air emboli in pigs. J Appl Physiol 1991; 71:1780–1786.
26. Altman DG. Practical statistics for medical research. London: Chapman and Hall, 1991:426–433.
27. Edmonds C, Lowry C, Pennefather J. Diving and subaquatic medicine, 3d ed. Oxford: Butterworth-Heinemann Ltd, 1992:152.
28. Verstappen FTJ, Bernards JA, Kreuzer F. Effects of pulmonary gas embolism on circulation and respiration in the dog. I. Effects on circulation. Pfluegers Arch Eur J Physiol 1977; 368:89–96.
29. Adornato DC, Gildenberg PL. Ferrario CM, Smart J, Frost EAM. Pathophysiology of intravenous air embolism in dogs. Anesthesiology 1978; 49:120–127.
30. Butler BD, Hills BA. Transpulmonary passage of venous air emboli. J Appl Physiol 1985; 59:543–547.
31. Nunn JF. Applied respiratory physiology. London: Butterworth, 1987.
32. Malik AB. Pulmonary microembolism. Physiol Rev 1983; 63:1114–1207.
33. Dalen JE, Haynes FW, Hoppin FG, Evans GL. Bhardwaj P, Dexter L. Cardiovascular responses to experimental pulmonary embolism. Am J Cardiol 1967; 20:3–9.
34. Hills BA, Butler BD. Size distribution of intravascular air emboli produced by decompression. Undersea Biomed Res 1981; 8:163–170.
35. Vik A, Jenssen BM, Brubakk AO. Arterial gas bubbles after decompression in pigs with patent foramen ovale. Undersea & Hyperbaric Med 1993; 20:121–132.
36. Ganong WF. Review of medical physiology, 15th ed. Englewood Cliffs, NJ: Prentice–Hall International, 1991:337–338.
37. Guyton AC, Jones CE, Coleman TG. Measurement of cardiac output by the direct Fick method. In: Circulatory physiology: cardiac output and its regulation, 2d ed. Philadelphia: WB Saunders, 1973:21–39.
38. Sawatzky KD, Nishi RY. Assessment of inter-rater agreement on the grading of intravascular bubble signals. Undersea Biomed Res 1991; 18:373–396.